

## Optimisation of Substrate Angles for Three Dimensional Inkjet Printing of multi-functional and multi-material parts

Jayasheelan Vaithilingam\*, Kasidis Laoboonmee, Ehab Saleh, Richard J.M. Hague, Ricky D. Wildman and Christopher J. Tuck

Additive Manufacturing and 3D-printing Research Group, EPSRC Centre for Innovative Manufacturing in Additive Manufacturing, Faculty of Engineering, University of Nottingham, Nottingham, UK. Postcode: NG9 2RD

### Abstract

Three dimensional (3D) inkjet printing of multiple materials is being explored widely to fabricate multi-functional parts such as the printing of strain gauges and heating elements embedded within a component. Although dielectrics and conductive materials can be inkjet-printed together, there is a difference in their layer thicknesses. Inkjet printed conductive materials require sintering at temperatures of around 150°C to form a conductive network. Exposing the dielectric materials which may be sensitive to prolonged heat exposure could affect their material properties. Hence, optimisation of conductive routes within the structural material is essential. It is envisaged that printing of structural materials at an angle to a certain height/layers and then printing a few layers (~ 10 layers) of conductive material on to the top surface will enable faster fabrication and reduced exposure of the dielectric material to heat. To compliment this aim, in this study, dielectric substrates were printed at different angles and the conductivity of the tracks were assessed. Surface morphology of the printed tracks showed misplacement of droplets for angles above 15° due to the influence of print height. The printed tracks remained conductive up to 65°; however above 50°, the tracks were highly resistive (> 150KΩ). The optimal angle to obtain conductive tracks with the highest print resolution was 15° and it was greatly influenced by the print height. Further study is required to optimise the substrate angle by using a constant print height and varying the slope length.

### Introduction

The use of three dimensional (3D) printing for the fabrication of multi-material and multi-functional printing is increasing. Wu et. al [1], used fused deposition modelling (FDM) to fabricate a ‘smart cap’ with embedded electronics. In this study, the part was printed with holes and a conductive paste was injected into the holes and sintered to form electrical interconnects. Shemelya et. al [2] fabricated multi-functional structures for satellite qualification by embedding electronics to a structure fabricated using FDM. However, there are limitations in using FDM to make one-step fully multi-functional parts with embedded electronics. The density of the FDM fabricated part is inferior to those manufactured by inkjet printing, in addition, the spatial resolution and the surface quality of the FDM fabricated parts may not be sufficient to fabricate sophisticated electronic components [3]. Also the porosity of FDM parts may potentially lead to short circuit if conductive tracks are printed.

The other key enabling 3D printing technique to make multifunctional 3D components is inkjet printing. However, the functionality of these multi-material parts is limited. For example, Inkjet printers such as those manufactured by Stratasys Objet® can make multi material parts using proprietary materials such as VeroClear®, TangoBlack® and TangoPlus®. Researchers have also used cartridges filled with different inks to produce multi-material parts. Zhang et. al [4] used two cartridges filled with polyimide ink and conductive silver nanoparticle (AgNP) ink to print a capacitor using Dimatix® inkjet printer. There are also several examples of inkjet printing of two dimensional structures for sensing applications in the literature [5–7].

Although there are several examples of inkjet printing electronic tracks, these are mainly limited to 2D structures or printed in 2D on a 3D structure. Inkjet printing of multiple materials to fabricate a 3D structure in a single step is a challenge as there is a limited range of materials that can be inkjet-printed. Also, most of the available materials are not thermally stable. Inks containing metal nanoparticles are widely used to form the conductive networks and sintering of these particles is essential for the functionality of the track [8]. To be able to sinter, the printed tracks have to be exposed to temperatures above 130°C; however, this greatly depends on the solvent and other additives within the ink [9]. Also a layer of sintered AgNPs tends to be approximately 10 times thinner than a polymeric structural material. So, while building a polymeric part containing a conductive track, the polymer will be exposed to the sintering temperature of silver 10 times for every layer of the polymer. Exposing the polymeric material to these temperatures could degrade the material if they are not thermally stable at these temperatures / cycles.

In this study, the possibility to print conductive tracks on an angular surface is explored. By printing a certain layers of conductive tracks at an angle, the ‘Z’ height can be reached faster than by printing the two materials in plane. Figure 1 shows the idea of how printing at an angle will be beneficial for multi-material 3D printing. The illustration on the left shows the conventional printing method where multiple layers of the conductive materials are printed and the illustration on the right depicts the proposed approach of printing few layers of conductive track. In order to attain this, the maximum angle up to which conductive tracks can be printed needs to be optimised and it is in focus of this study.

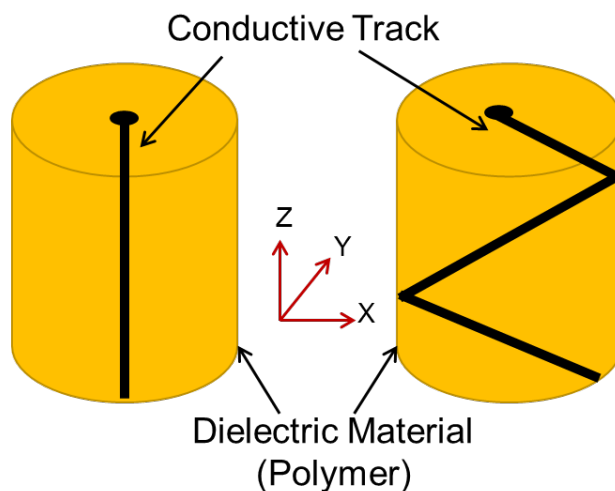


**Figure 1** Illustration of conventional printing and the proposed angular approach to print conductive tracks on a dielectric polymeric material.

## 2. Materials and Methods

### 2.1. Materials

Conductive AgNP ink was purchase from Advanced Nano Products (ANP), Korea. SYS, UK supplied VeroClear<sup>®</sup> and SUP705<sup>®</sup> for building parts in an Objet<sup>®</sup> Connex 260. Isopropyl alcohol (IPA)  $\leq 99.5\%$  was purchased from Sigma Aldrich, UK. Conductive paint and Kapton<sup>®</sup> tape was supplied by RS Components, UK.

## 2.2. Methods

### 2.2.1. Design

Creo® Parametric computer aided design (CAD) software was used to design parts with angles ranging from 0° to 65°. The conductive track pattern was designed using the General Image Manipulation Program (GIMP) with a resolution was 846.67 dpi. The dimensions of the tracks are shown in Figure 2.

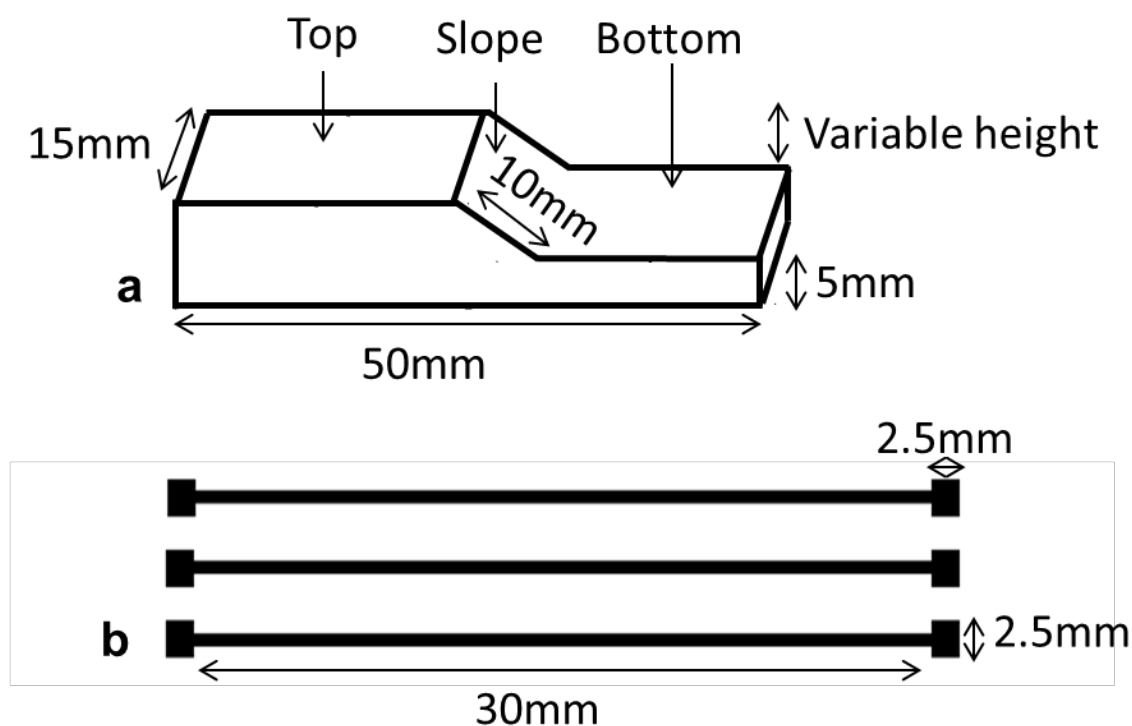


**Figure 2** Dimensions of the (a) part printed with varied substrate angles and the (b) 1mm wide conductive tracks printed on them.

### 2.2.2. 3D printing

Samples with angles ranging from 0° to 70° were fabricated using Objet® Connex 260. VeroClear® was used as the build material and SUP705 was used as the support material. Briefly, the CAD model of the parts were arranged in the build platform parallel to the print direction. The in-built Spectra SE128 (Fujifilm, USA) print head was cleaned before printing using IPA and the set condition of the printer was used to print the pattern. After printing, the VeroClear® samples were removed from the build plate. The supports were removed manually and the samples were cleaned using IPA and deionised water and dried. The cleaned VeroClear® sample was placed in a Dimatix® DMP2831 (Fujifilm, USA) and secured with a Kapton® tape. A 10pL cartridge was filled with AgNP ink. The calculated drop spacing was 30µm and hence the print head was adjusted to an angle of 6.8°, as recommended by the manufacturer to achieve the appropriate dpi. Print height was set at 1mm from the top surface and the firing voltage was 27 V. Cartridge temperature was set to 30°C. The print pattern was aligned to the VeroClear® surface by the use of a fiducial camera. Working nozzles were selected and in this case, since the ink was stable, all nozzles (1 – 16) were selected to print. Once a layer was complete, the ink was dried using a hot air drier approximately 15mm from the surface of the sample. This was performed to dry solvents in the ink and the next layer was printed. This procedure was repeated until the required number of layers was printed. After

printing final layer, the sample was transferred to a convection oven operating at 130°C for 30 mins. This was performed to sinter the AgNPs in the printed tracks.

### 2.2.3. Characterisation

The printed VeroClear<sup>®</sup> substrate and conductive tracks printed on them were examined using a Nikon Eclipse (LV100ND) optical microscope. The surface profile of the tracks was obtained using a SurfTest SV-600 (Mitutoyo, UK) contact probe surface profilometer. Electrical resistance of the tracks were obtained using a Hameg<sup>®</sup> LCR high precision meter (HM 8018) supplied by Rhode and Schwarz, UK.

## 3. Results and Discussion

Surface morphology of the printed VeroClear<sup>®</sup> sample showed an undulating morphology (Figure 3a), which was also confirmed by surface profilometry (Figure 3b). Previous research showed a similar morphology for inkjet printed polymeric surfaces [4].

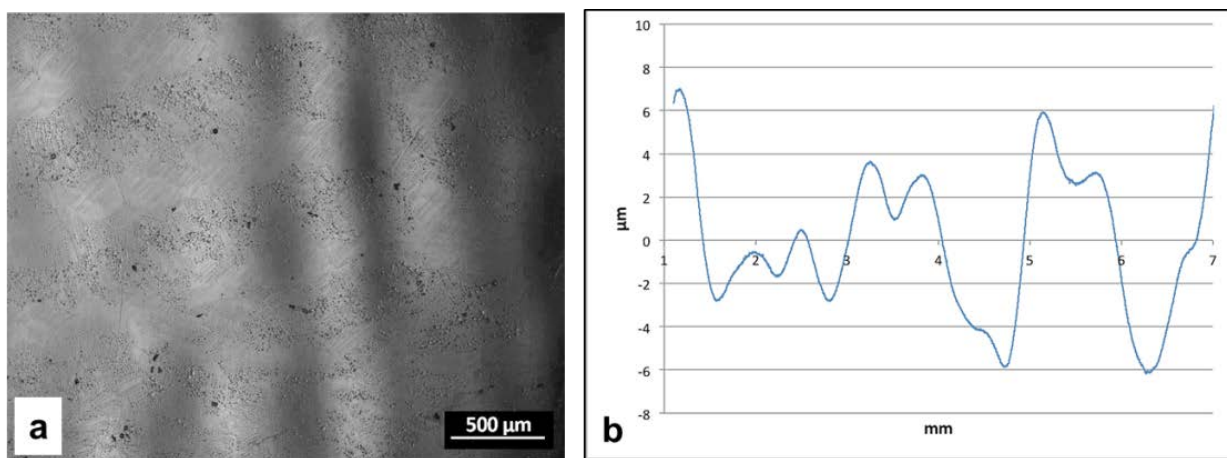


**Figure 3** (a) surface morphology of the printed VeroClear<sup>®</sup> part and (b) the corresponding surface profile.

Figure 4 shows samples with varied angles and the conductive tracks printed and sintered on the surface. On examining the surface morphology of these printed silver tracks, the top surface was observed to show similar surface morphology for the samples with all angles i.e. 0° - 65°. The droplets were precisely placed on the VeroClear<sup>®</sup> surface according to the print pattern. The bottom part of the sample showed a similar morphology up to 15°. Beyond this angle, the bottom surface showed a significant difference in the morphology with the increase in angle. As it can be observed from Figure 5, the print resolution of the tracks for samples with higher angle was poorer when compared to the resolution obtained for lower angles (up to 15°). The primary reason for this difference is due to the increase in print height with respect to the angle of the slope to the surface. The increase in print height with respect to the increase in angle has been shown in Table 1. It can be observed that at 20°, the substrate is 6mm away from the sample and hence a slight drift in the droplets from the trajectory can be observed (Figure 6). Further increasing the substrate angle above 20°, increased print height causing a further drag, drifting the droplets away from the print area. Similar effect due to the droplet aerodynamics for the drop-on-demand printing system have been previously reported in literature [10]. Hence the silver tracks printed on 65° sample showed the highest disorientation of droplets compared to other lower angles.

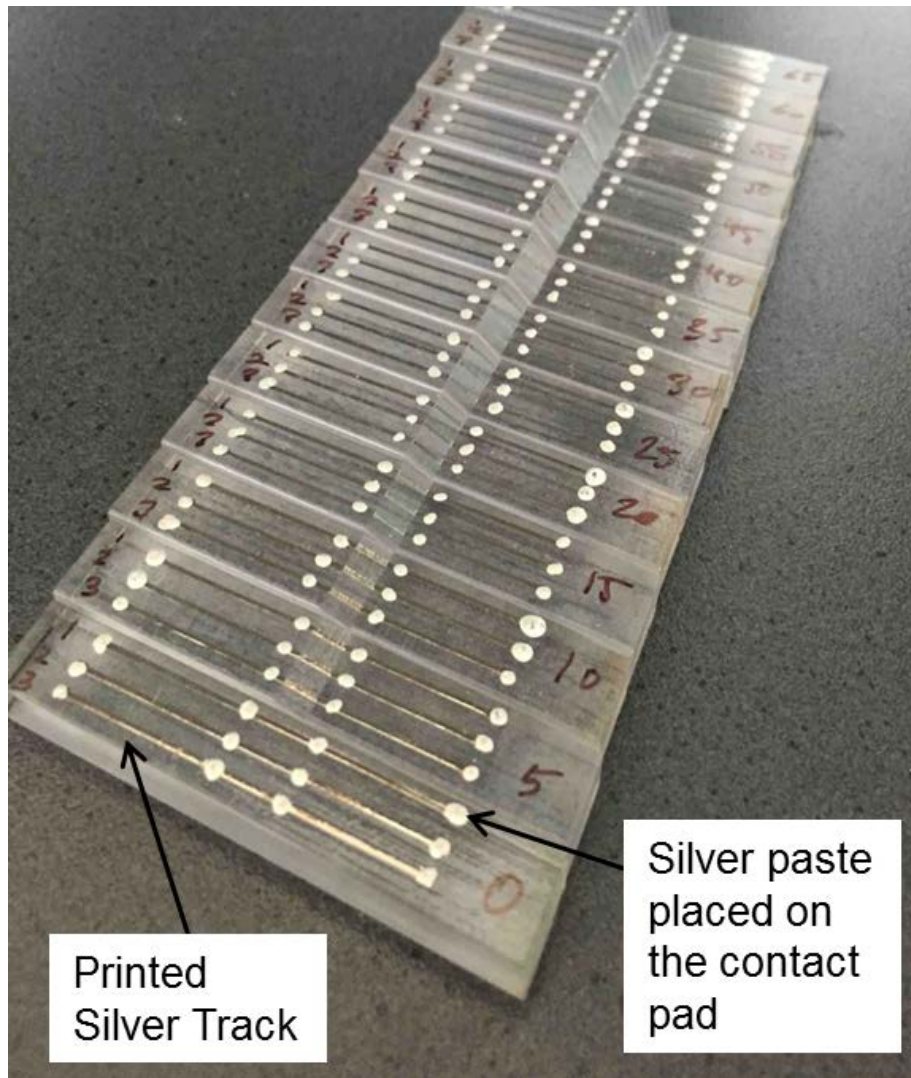


**Figure 4** Conductive tracks printed on the VeroClear® substrate at various substrate angles.

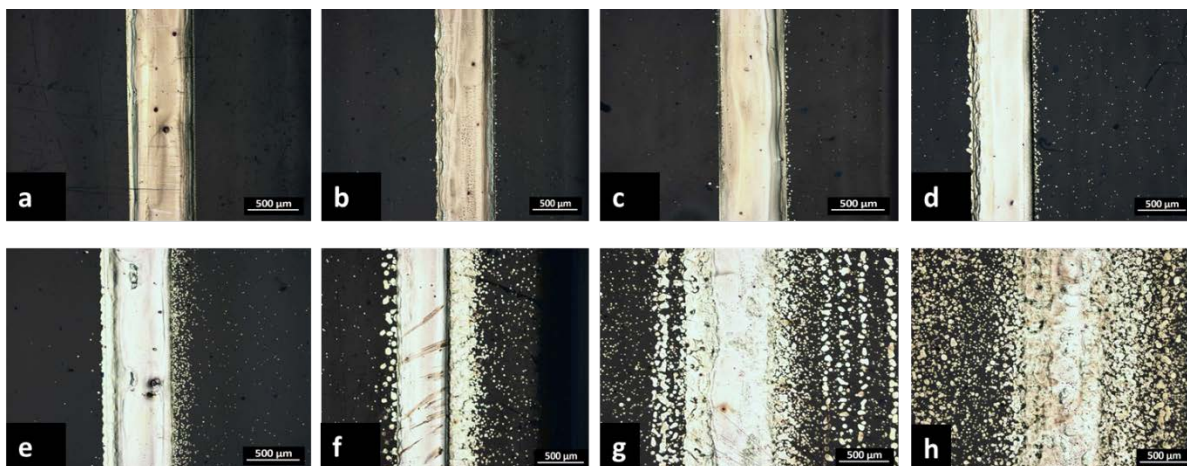


**Figure 5** Surface morphology of the printed silver tracks on substrates (bottom) with (a) 0°, (b) 5°, (c) 15°, (d) 25°, (e) 35°, (f) 45°, (g) 55°, (h) 65°. Scale bar represents 500μm.

**Table 1** Print height used for the top and bottom surfaces

Angle (°)	Print Height	
	Top Surface (mm)	Bottom Surface (mm)
0	1	1
5	1	3.1
10	1	4.1
15	1	5
20	1	5.9
25	1	6.8
30	1	7.7
35	1	8.5
40	1	9.2
45	1	9.9
50	1	10.5
55	1	11.1
60	1	11.5
65	1	12
70	1	12.2

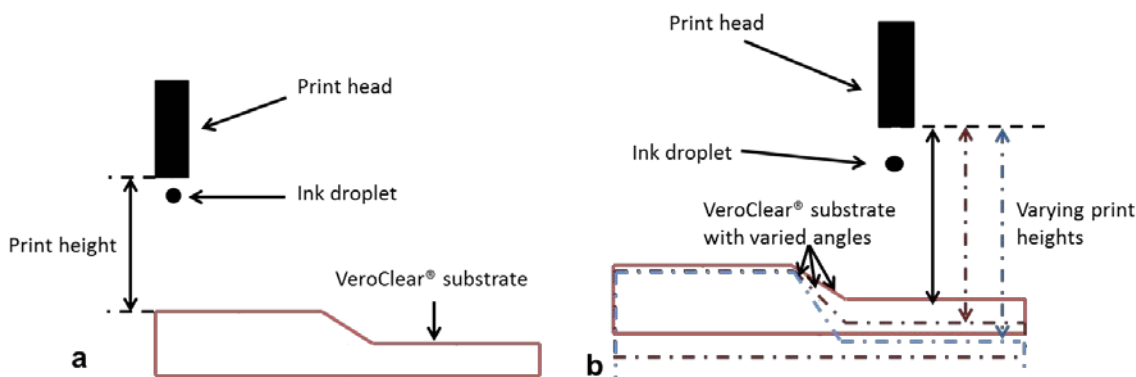


**Figure 6** Illustration of the print height on (a) top surface and (b) bottom surface.

The electrical resistance of the tracks printed on VeroClear<sup>®</sup> was measured to determine the maximum angle at which the track loses its conductivity. Figure 7 shows the resistance of the track with respect to the substrate angle in log scale. The printed conductive tracks on the VeroClear<sup>®</sup> substrate remained conductive until 65° and beyond this angle no conductance was noted. It can be observed that up to the angle of 50°, the resistance of the printed tracks did not vary significantly; however beyond this angle, the tracks were highly resistive. The deviation of the values from the mean was also high, revealing the inconsistencies in the printed tracks. The major reasons for this increased resistance are the substrate angle and the print height. As the angle was steep, there is an opportunity for the ink droplets to flow to the bottom of the surface, leaving less ink on the upper portion of the track. Also, due to the increased print height at these angles, the placement of droplets was difficult due to the drag and drifting of the droplets from its trajectory.

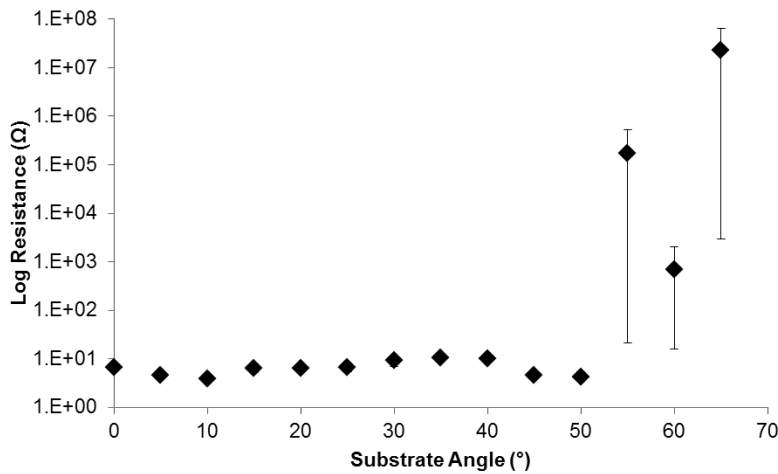


**Figure 7** Logarithmic resistance measured for the printed silver tracks on substrates with varied angle.

Due to the observed distortion in the printed pattern, the track was divided into top, slope and the bottom area and the individual resistance on these areas was measured. As it can be observed from Figure 8, the electrical resistance on the top, slope and the bottom surfaces did not show a significant difference with respect to the increase in the angle up to 50°. Also the deviation of the results from the mean was low compared to the samples with angles above 50°. However, for the tracks printed on substrates above 50°, the resistance of the tracks printed on the slope increased significantly. This clearly shows that the substrate angle plays a crucial role in the conductivity of the printed silver track on the angular surfaces. Also the resistance measured on the bottom area of the samples showed an increasing trend above 50°. This is primarily due to the scattering of droplets around the print area; however these resistances were much lower than that of the resistance of the slope.

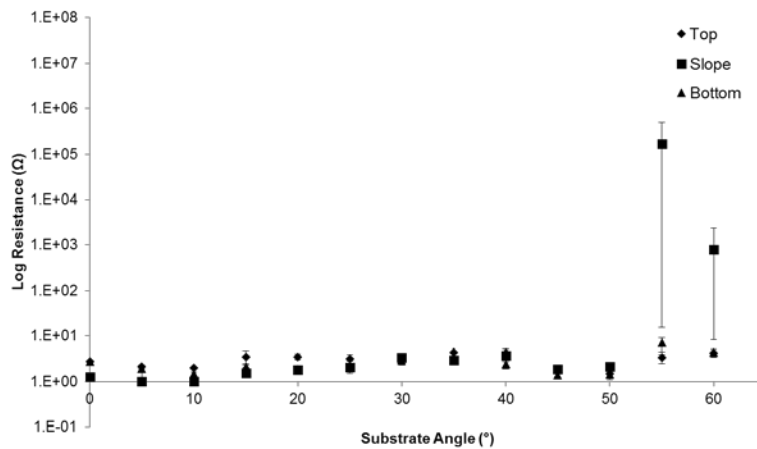


**Figure 8** Resistance measured for the isolated silver tracks (top, slope and bottom areas) on substrates with angles up to 65° in logarithmic scale.

The presented results showed that both the substrate angle and the print height have a significant influence on the track resistance and morphology. Although the tracks remained conductive up to 65°, the resistance of the track was high and fluctuating above 50°. Despite the low resistance (up to 10Ω) of the tracks printed until 50°, the resolution of the printed pattern was poor for substrate angle above 15°. Printing above 15° can impose a restriction on the feature size and the resolution. Considering the feature size, resolution and the resistance,

printing at 15° seems an acceptable compromise to increase print efficiency. Since print height plays a crucial role on the placement of droplets, print height can be fixed and the length of the slope may be altered. By performing this way, tracks with a good resolution can be achieved and may possibly enable printing at angles above 15°.

In order to build a 4mm cylinder with a conductive track, for building both in a plane, it would require 5000 layers of silver assuming the layer thickness as 800nm. However by printing in 15°, 10 layer is sufficient to reach this Z height. The time to print and sinter 4990 layers will be saved by using this approach when printing and sintering continuously.

#### **4. Conclusion**

Printing conductive tracks on angular substrates up to 65° is possible; however, the resistance of the track increased with the increase in substrate angle. Printing at 15° was observed to be the optimum angle for printing of conductive tracks on 3D structures. Placement of droplets was significantly affected by the print height. Hence optimization of print height is essential. This optimized angle can be used to print conductive tracks and attain the 'Z' height faster than printing in plane.

#### **Acknowledgement**

The authors gratefully acknowledge funding support from the Engineering and Physical Sciences Research Council (EPSRC), [UK] under the EPSRC Centre for Innovative Manufacturing in Additive Manufacturing (EP/I033335/2) at the University of Nottingham, UK. The authors also acknowledge the technical assistance offered by the technicians Mr. Mark East, Mr. Mark Hardy and Mr. Joe White at the Additive Manufacturing and 3D Printing Research Group (AM&3DPRG), University of Nottingham.

#### **References**

1. Wu S-Y, Yang C, Hsu W, Lin L. 3D-printed microelectronics for integrated circuitry and passive wireless sensors. *Microsystems Nanoeng.* 2015;1:15013.
2. Shemelya C, Banuelos-chacon L, Melendez A, Kief C, Espalin D, Wicker R. Multi-functional 3D Printed and Embedded Sensors for Satellite Qualification Structures. *Sensors.* Ieee; 2015;1–4.
3. Espalin D, Muse DW, MacDonald E, Wicker RB. 3D Printing multifunctionality: Structures with electronics. *Int. J. Adv. Manuf. Technol.* 2014;72:963–78.
4. Zhang F, Tuck C, Hague R, He Y, Saleh E, Li Y, et al. Inkjet Printing of Polyimide Insulators for the 3D Printing of Dielectric Materials for Microelectronic Applications. *J. Appl. Polym. Sci.* 2016;133(18).
5. Vyas R, Lakafosis V, Lee H, Shaker G, Yang L, Orecchini G, et al. Inkjet printed, self powered, wireless sensors for environmental, gas, and authentication-based sensing. *IEEE Sens. J.* 2011;11(12):3139–52.
6. Molina-Lopez F, Briand D, De Rooij NF. All additive inkjet printed humidity sensors on plastic substrate. *Sensors Actuators, B Chem.* 2012;166-167:212–22.
7. Bidoki SM, Lewis DM, Clark M, Vakorov a, Millner P a, McGorman D. Ink-jet fabrication of electronic components. *J. Micromechanics Microengineering.* 2007;17(5):967–74.

8. Yin ZP, Huang Y a., Bu NB, Wang XM, Xiong YL. Inkjet printing for flexible electronics: Materials, processes and equipments. *Chinese Sci. Bull.* 2010;55(30):3383–407.
9. Niittynen J, Abbel R, Mäntysalo M, Perelaer J, Schubert US, Lupo D. Alternative sintering methods compared to conventional thermal sintering for inkjet printed silver nanoparticle ink. *Thin Solid Films*; 2014;556:452–9.
10. Castrejon-Pita J, Baxter W. Future , Opportunities and Challenges of Inkjet Technologies. *At. Sprays.* 2013;23(6):541–65.